

Electronic Supporting Information

Syntheses, structures and properties of three organic-inorganic hybrid polyoxotungstates constructed from {Ni₆PW₉} building blocks: from isolated cluster to 2-D layer

Zhong Zhang, Yue-Lin Wang, Hai-Lou Li, Ke-Ning Sun, and Guo-Yu Yang*

MOE Key Laboratory of Cluster Science, School of Chemistry and Chemical Engineering, Beijing Institute of Technology, Beijing 100081, China. E-mail: ygy@bit.edu.cn, Fax: (+86) 10-6891-8572

Table S1. Bond valence sum (BVS) calculations of all Ni, P and W atoms in **1-3**.

Table S3. The select H-bond lengths with the atomic number in **1-2**.

Figure S1. Structure of {Ni₆PW₉(H₂O)₆}.

Figure S2. The comparisons of PXRD spectra of **1-3** with the simulated X-ray diffraction patterns based on single-crystal structural analysis.

Figure S3. a) The double layer group in **3**; b) simplified representation of double layer; c) view of the stacking fashion in **3**.

Figure S4. IR spectra of **1-3**.

Figure S5. The TG curves of **1-3**.

Figure S6. (a) The variation of CVs of **3**-CPE in pH = 1.75 0.5 mol L⁻¹ Na₂SO₄/H₂SO₄ aqueous solution with the amount of different H₂O₂ (0; 9 × 10⁻⁴; 1 × 10⁻³; 3 × 10⁻³; 5 × 10⁻³; 7 × 10⁻³; 9 × 10⁻³ mol L⁻¹); (b) the variation of CVs of **3**-CPE in pH = 1.75 0.5 mol L⁻¹ Na₂SO₄/H₂SO₄ aqueous solution with the amount of different NaNO₂ (0; 9 × 10⁻⁴; 1 × 10⁻³; 3 × 10⁻³; 5 × 10⁻³; 7 × 10⁻³; 9 × 10⁻³ mol L⁻¹). Scan speed: 30 mV s⁻¹.

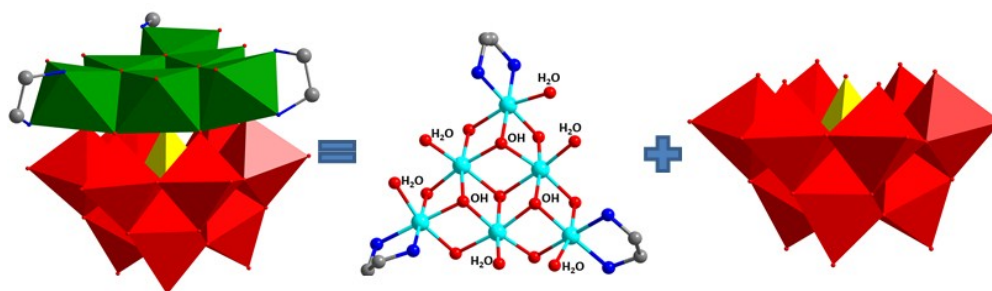
Figure S7. Plots of Kunelka-Munk function versus energy E (eV) for **1-3**.

Table S1. Bond valence sum (BVS) calculations of all Ni, P and W atoms in **1-3**.

1-BVS				2-BVS				3-BVS			
Ni1	2.00	W2	5.98	Ni1	2.01	W2	6.17	Ni1	2.09	W3	6.13
Ni2	2.01	W3	6.35	Ni2	2.06	W3	6.17	Ni2	2.06	W4	6.14
Ni3	2.02	W4	5.89	Ni3	2.07	W4	6.11	Ni3	1.92	W5	6.21
Ni4	1.92	W5	5.97	Ni4	2.10	W5	6.10	Ni4	2.08	W6	6.04
Ni5	2.11	W6	6.18	Ni5	1.98	W6	6.30	Ni5	1.91		
Ni6	1.92	W7	6.10	Ni6	1.99	W7	6.23	P1	5.02		
Ni7	2.02	W8	6.28	Ni7	2.49	W8	6.09	P2	5.16		
P1	5.07	W9	5.93	P1	4.90	W9	6.20	W1	5.91		
W1	6.00			W1	6.20			W2	6.02		

Table S2. The select H-bonds in **1-2**.

Donor-H---Acceptor	D-H	H...A	D...A
1			
N9-H9A...O33	0.86	2.53	3.0590
N9-H9B...O4W	0.86	1.93	2.7720
O4W-H4WA...O17	0.85	1.96	2.8095
N4W-H4WB...O39	0.85	2.07	2.9219
2			
O17-H17A...O25	0.85	1.87	2.675
O24-H24A...O33	0.85	2.38	3.223
O17-H17A...O25	0.85	1.87	2.675
O24-H24A...O33	0.85	2.38	3.223

**Figure S1.** Structure of $\{\text{Ni}_6\text{PW}_9(\text{H}_2\text{O})_6\}$.

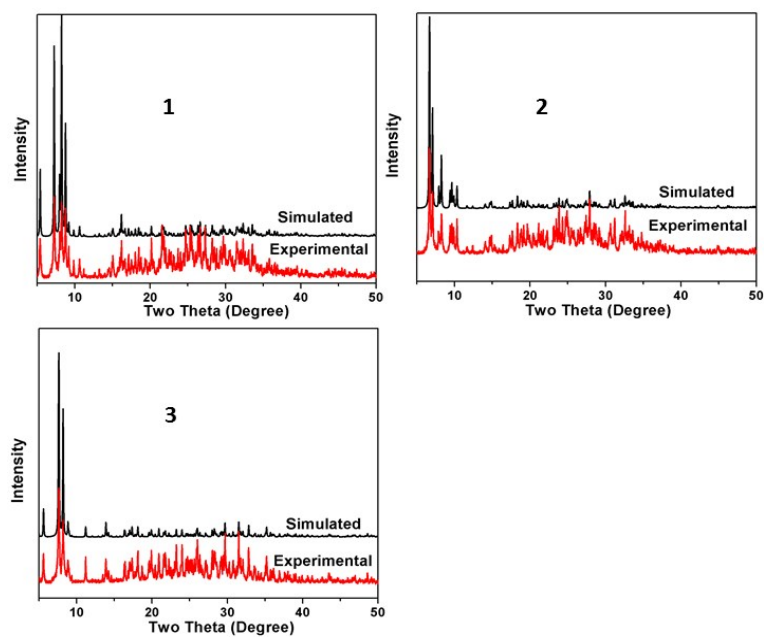


Figure S2. The comparisons of PXRD spectra of **1-3** with the simulated X-ray diffraction patterns based on single-crystal structural analysis.

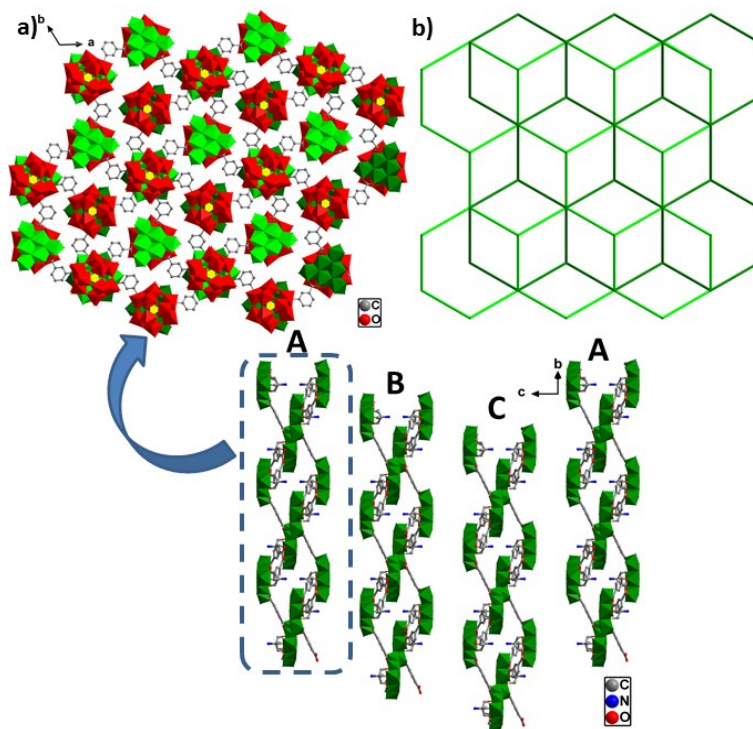


Figure S3. a) The double layer group in **3**; b) simplified representation of double layer; c) view of the stacking fashion in **3**.

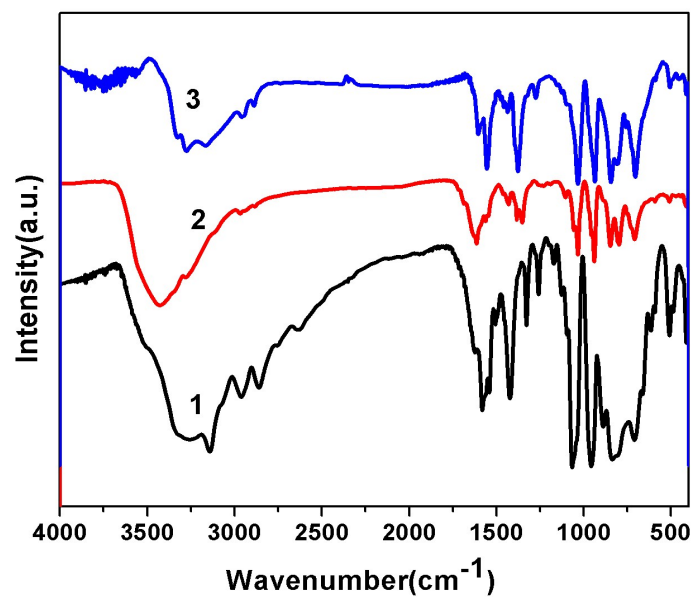


Figure S4. IR spectra of 1-3.

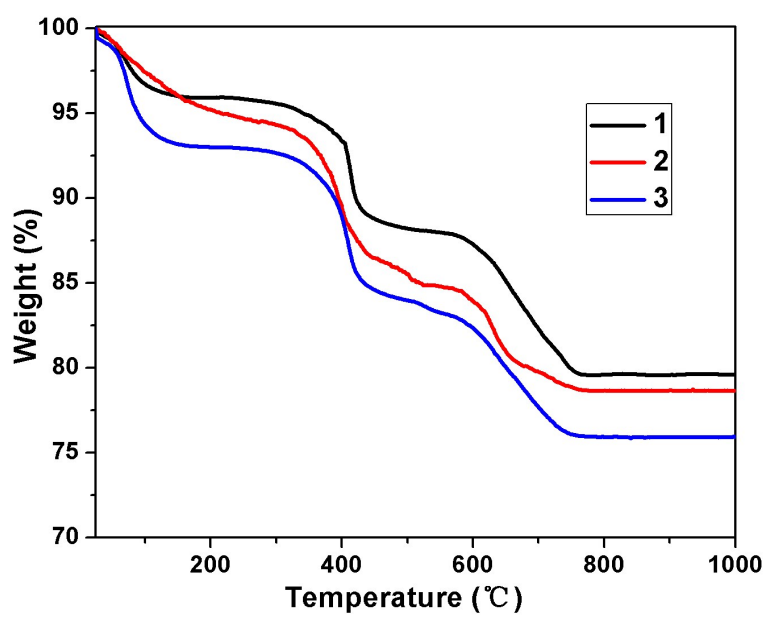


Figure S5. The TG curves of 1-3.

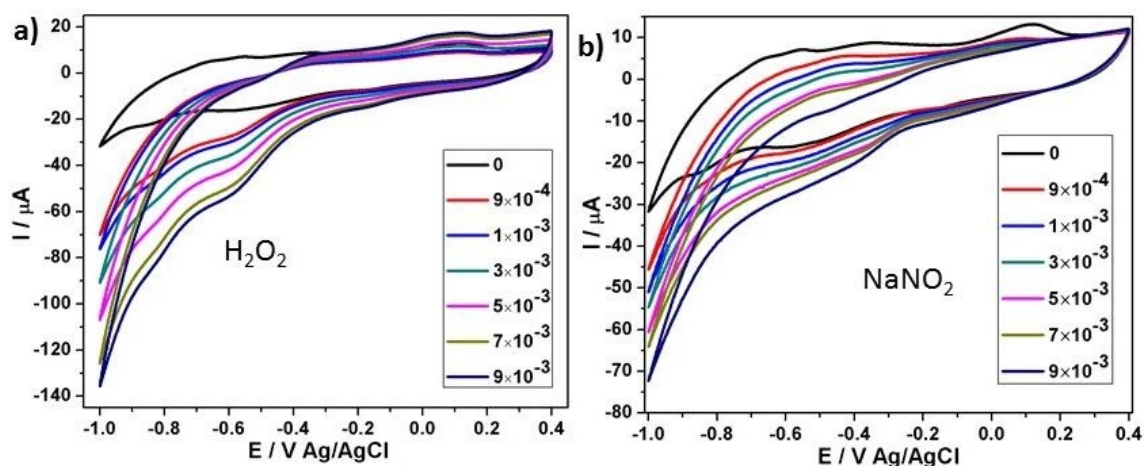


Figure S6. (a) The variation of CVs of **3-CPE** in pH = 1.75 0.5 mol L⁻¹ Na₂SO₄/H₂SO₄ aqueous solution with the amount of different H₂O₂ (0; 9 × 10⁻⁴; 1 × 10⁻³; 3 × 10⁻³; 5 × 10⁻³; 7 × 10⁻³; 9 × 10⁻³ mol L⁻¹); (b) the variation of CVs of **3-CPE** in pH = 1.75 0.5 mol L⁻¹ Na₂SO₄/H₂SO₄ aqueous solution with the amount of different NaNO₂ (0; 9 × 10⁻⁴; 1 × 10⁻³; 3 × 10⁻³; 5 × 10⁻³; 7 × 10⁻³; 9 × 10⁻³ mol L⁻¹). Scan speed: 30 mV s⁻¹.

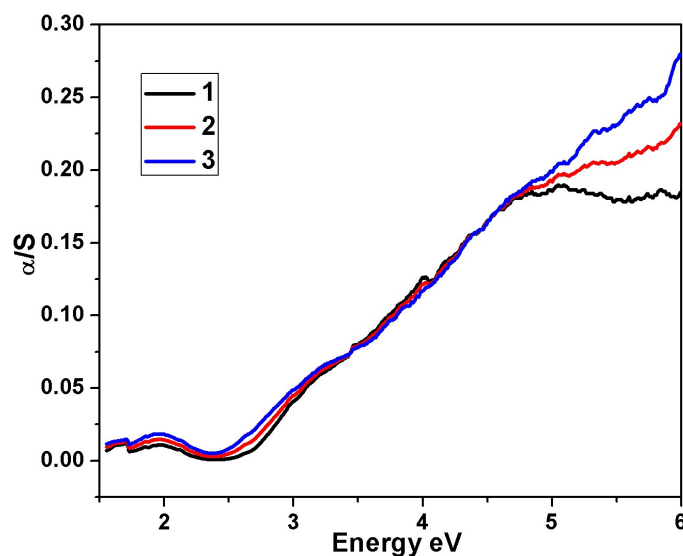


Figure S7. Plots of Kubelka-Munk function versus energy E (eV) for **1-3**.

The diffuse reflectance spectrum of **1-3**.

To explore the semi-conductivity of **1-3**, the measurements of diffuse reflectance spectrum for powdered crystal sample was performed to obtain their band gaps (E).¹ The band gap (E) was determined as the intersection point between the energy axis and the line extrapolated from the linear portion of the absorption edge in a plot of Kubelka-Munk function against energy E. Kubelka-Munk function $\alpha/S = (1-R)^2/2R$, was converted from the recorded diffuse reflectance data, where α is the absorption coefficient, S is the scattering coefficient, R is the reflectance of an infinitely thick layer at a given wavelength. The plot of Kubelka-Munk function versus energy E (eV) for **1-3** is shown in [Figure S7](#). Their band gaps E are 2.62, 2.53 and 2.42 eV for **1-3**, respectively. These band gaps are related to the energy-level difference between the oxygen p-type

HOMO and the tungsten p-type LUMO.² Similar behaviors have been observed in several reported Ni₆-substituted POMs, such as [$\{\text{Ni}_6(\mu_3\text{-OH})_3(\text{en})_2(\text{H}_2\text{O})_8\}(\text{PW}_9\text{O}_{34})$] (en = ethylenediamine),³ [$\text{Ni}(\text{enMe})_2$]₃(WO₄)₃[$\text{Ni}_6(\text{enMe})_3(\text{OH})_3\text{PW}_9\text{O}_{34}$]₂ (enMe = 1,2-diaminopropane).⁴ Obviously, it was found that the band gaps E of **1-3** follow the order of **3**<**2**<**1**, which conforms to the band gaps of the compounds decrease with increasing dimensionality or complexity of the structures, as pointed out by Kanatzidis and Papavassiliou.⁵

- 1 (a) W. M. Wesley and W. G. H. Harry, Reflectance Spectroscopy, Wiley (New York, 1966);
(b)
J. I. Pankove, Optical Processes in Semiconductors, Prentice-Hall (New York, 1997).
- 2 Y. Xia, P. Wu, Y. Wei, Y. Wang and H. Guo, Cryst. Grow. Des., 2006, **6**, 253.
- 3 J. W. Zhao, H. P. Jia, J. Zhang, S. T. Zheng and G. Y. Yang, Chem. -Eur. J. 2007, **13**, 10030.
- 4 X. X.Li, W. H. Fang, J. W. Zhao and G. Y. Yang, Chem. Eur. J. 2014, **20**, 17324.
- 5 E. A. Axtell, Y. Park, K. Chondroudis and M. G. Kanatzidis, J. Am. Chem. Soc., 1998, 120, 124.